# AD-A283 859

PAGE

| 1 AGENCY USE ONLY | 2 REPORT DATE 1994 | 3 TYPE/DATES COVERED |
|---|---|---|
| 4 TITLE AND SUBTITLE   Resistance to Penetration and Compression of Fibre-reinforced composite materials | | 5 FUNDING NUMBERS |
| 6 AUTHOR   R L WOODWARD, G T EGGLESTONE, B J BAXTER AND K CHALLIS | | |
| 7 FORMING ORG NAMES/ADDRESSES  DEFENCE SCIENCE AND TECHNOLOGY ORGANIZATION, MATERIALS RESEARCH LABORATORY, PO BOX 50, ASCOT VALE VICTORIA 3032  AUSTRALIA | | 8 PERFORMING ORG. REPORT NO |
| 09 SPONSORING/MONITORING AGENCY NAMES AND ADDRESSES | | |
| 11 SUPPLEMENTARY NOTES | | |
| 12 DISTRIBUTION/AVAILABILITY STATEMENT  DISTRIBUTION STATEMENT A | | 12B DISTRIBUTION CODE |

13. ABSTRACT (MAX 200 WORDS):TESTS ON BALLISTIC PENETRATION, QUASI-STATIC AND DYNAMIC CONSTRAINED COMPRESSION TESS AND TENSILE TESTS ARE REPORTED FOR GLASS-REINFORCED PLASTIC (GRP) KEVLAR, NYLON AND POLYETHYLENE COMPOSITES.  SECTIONING OF TESTED SAMPLES ALLOWED DEFORMATION MECHANISMS TO BE STUDIED.  BALLISTIC PENETRATION IS ASSOCIATED WITH FIBRE TENSILE FAILURE AND BALLISTIC RESISTANCE CORRELATES WITH TENSILE MODULUS.  HOWEVER, NO CORRELATION BETWEEN THE LEVELS OF FRACTURE STRESS OR FRACTURE STRAIN AND BALLISTIC RESISTANCE WAS FOUND TO EXIST.  tHE MECHANISMS OF DEFORMATION DEPEND ON COMPOSITE TYPE AND DIFFERENCES CAN EXIST BETWEEN DYNAMIC AND STATIC TESTS ON IDENTICAL SPECIMENS.  ENERGY ABSORPTION IN PENETRATION OF ORGANIC-FIBRE COMPOSITES IS BY FIBRE STRETCHING.  PENETRATION OF GRP COMPOSITES INVOLVES FIBRE AND MATRIX CRUSHING AND EXTRUSION.

| 14 SUBJECT TERMS | 15 NUMBER OF PAGES 22 |
|---|---|
| | 16 PRICE CODE |

| 17 SECURITY CLASS.REPORT  UNCLASSIFIED | 18 SEC CLASS PAGE UNCLASSIFIED | 19 SEC CLASS ABST. UNCLASS | 20 LIMITATION OF ABSTRACT |
|---|---|---|---|

94 8 25 4

94-27247

# RESISTANCE TO PENETRATION AND COMPRESSION OF FIBRE-REINFORCED COMPOSITE MATERIALS[†]

R. L. Woodward, G. T. Egglestone, B. J. Baxter and K. Challis

DSTO Materials Research Laboratory, PO Box 50, Ascot Vale, Victoria 3032, Australia

**Abstract**—Tests on ballistic penetration, quasi-static and dynamic constrained compression tests and tensile tests are reported for glass-reinforced plastic (GRP), Kevlar®, nylon and polyethylene composites. Sectioning of tested samples allowed deformation mechanisms to be studied. Ballistic penetration is associated with fibre tensile failure and ballistic resistance correlates with tensile modulus. However, no correlation between the levels of fracture stress or fracture strain and ballistic resistance was found to exist. The mechanisms of deformation depend on composite type and differences can exist between dynamic and static tests on identical specimens. Energy absorption in penetration of organic-fibre composites is by fibre stretching. Penetration of GRP composites involves fibre and matrix crushing and extrusion.

## INTRODUCTION

Perforation of composites by a projectile travelling at ballistic velocity involves a number of mechanisms whose contribution to kinetic-energy absorption and ballistic resistance changes with time (Egglestone *et al.*, 1990; Ayaz *et al.*, 1991). For a target of finite thickness, initial impact results in acceleration, and consequent compression of material ahead of the projectile. This is followed by interfacial delamination, stretching and bending of the composite as the projectile approaches the rear side of the target. In metallic composites where plastic deformation results in a permanent set, post-penetration measurements can be used to elucidate the distribution of energy amongst the different processes (Woodward *et al.*, 1991). Modelling and simulation tests aid in the understanding and prediction of penetration behavior (Woodward and deMorton, 1976; Woodward, 1982; Woodward and Crouch, 1989; Crouch and Woodward, 1989). For fibre-reinforced composites, high-speed cine techniques which provide time-resolved profile geometry and velocity data can also assist in understanding the mechanisms of energy absorption (O'Donnell, 1994; Morrison and Bowyer, 1980; Zhu *et al.*, 1992). Savage (1990) has reviewed factors which influence the penetration resistance of fibre-reinforced composites and the physical requirements of applications.

The present work concentrates on compressive deformation of fibre-reinforced composite laminates, which is relevant to the early stage of penetration in thin targets and is a dominant mechanism for thick targets. The work is directed at understanding some of the fundamentals of deformation, hence the effort to design simplified model experiments rather than the conventional approach of examining perforation of the targets. Values for penetration resistance are determined by ballistic impact of semi-infinite targets which are then sectioned to study the process of deformation. Resistance to compression is measured independently using a Hopkinson bar for constrained dynamic compression tests (Woodward and deMorton, 1976; Woodward, 1982; Crouch and Woodward, 1989). Studies of these dynamic properties are compared with similar quasi-static compression and tensile test data.

## MATERIALS AND TESTING METHODS

The details of fabric construction, resin type and fibre-volume fractions are given in Tables 1 and 2. In all cases the fabric reinforcement was of a plain woven construction and the nominal fibre-volume fractions were: 60% for S2 glass-reinforced laminates, 74%

[†] Copyright Commonwealth of Australia.

Table 1. Composites tested for compression and penetration

| Material | Fibre | Fabric construction (Ends cm⁻¹) | Fabric construction (Picks cm⁻¹) | Fibre-volume fraction (%) | Resin/bond | Construction | Nominal thickness (mm) |
|---|---|---|---|---|---|---|---|
| GRP | S2 Glass | 2 | 2 | 60 | Polyester A2785CV | 12 Plies | 6.2 |
| Kevlar® | Kevlar® 29 | 7 | 7 | 78 | Phenol formaldehyde Polyvinyl butyral | 19 Plies | 9.2 |
| Nylon | Ballistic nylon | 14 | 13 | 74 | Polyester A2785CV | 22 Plies | 7.4 |
| Polyethylene | Spectra® 1000 | 13 | 13 | 62 | Polyester A2785CV | 20 Plies | 6.0 |

Table 2. Composites for tension tests

| Material | Fibre | Fabric construction (Ends cm⁻¹) | Fabric construction (Picks cm⁻¹) | Fibre-volume fraction (%) | Resin/bond | Construction | Nominal thickness (mm) |
|---|---|---|---|---|---|---|---|
| GRP | S2 Glass | 2 | 2 | 61 | Polyester A2785CV | 7 Plies | 4.1 |
| Kevlar® | Kevlar® 29 | 7 | 7 | 69 | Vinylester 8084 | 14 Plies | 8.1 |
| Nylon | Ballistic nylon | 14 | 13 | 70 | Vinylester 8084 | 22 Plies | 8.3 |
| Polyethylene | Spectra® 1000 | 13 | 13 | 75 | Vinylester 8084 | 5 Plies | 1.3 |

for Kevlar®, 72% for ballistic nylon and 75% for Spectra. For ballistic tests against semi-infinite targets only the glass-reinforced plastic (GRP), Kevlar® and nylon composites were used due to the difficulty in maintaining interlaminar bonding between the polyethylene fibres and resin during ballistic tests. The minimum dimensions of the semi-infinite targets tested were 150 mm square and 150 mm thick.

Ballistic testing of the semi-infinite targets was achieved by firing a hard, flat-ended cylindrical steel projectile of diameter 12.7 mm and mass 24.0 g into the composite. A flat-ended projectile was chosen because it is against such projectiles that composite targets of the present type achieve their maximum performance, and because their major use is to stop fragments which can be idealized as flattened projectiles. For a non-deforming penetrator, the indicator of ballistic resistance or the mean pressure resisting penetration, $P$, is related to the depth of penetration, $d$, and the impact kinetic energy by

$$PAd = \tfrac{1}{2}mv^2 \qquad (1)$$

where $A$ is the projectile cross-sectional area,
  $m$ is the projectile mass,
and $v$ is the impact velocity.

The depth was determined by depth gauging the hole and also by measurements after post-impact sectioning of the target. Because eqn (1) is derived by equating the total work done to the impact kinetic energy, the average value of pressure obtained does not depend on what mechanism or mechanisms are involved, and all deformation work terms are included, i.e. fracture, elastic and plastic flow, heating, friction etc. By assuming the work of penetration is dissipated in elastic stretching of the surrounding fibres, the radius, $r$, to which the fibres are stretched to their breaking strain, $\varepsilon_f$, can be estimated from

$$r = \varepsilon_f^{-1}(mv^2/\pi Ed)^{-0.5} \qquad (2)$$

where $E$ is the elastic tensile modulus of the fibre.

This equation assumes a cylindrical volume of stretched fibres, with a depth equal to that of penetration, $d$. The analysis is only relevant if radial stretching of the fibres is the mechanism, and then assumes uniform strain in the extended portion of fibre. The lack of accurate knowledge of dynamic fracture strain and dynamic modulus data, combined with these assumptions, emphasises that $r$ is an estimate only.
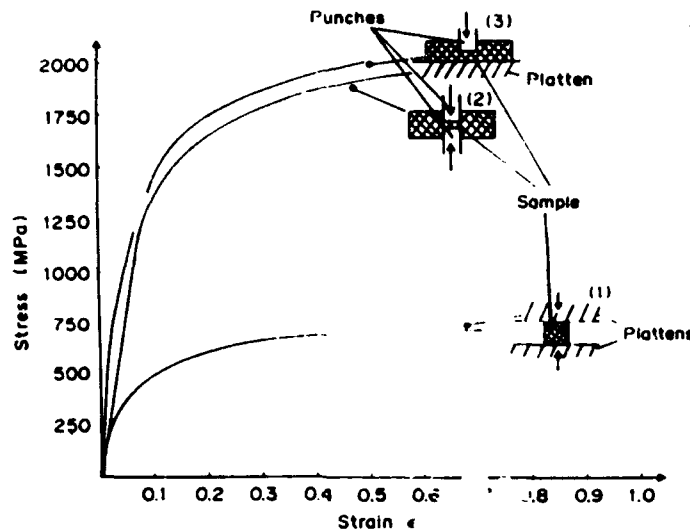
Fig. 1. Compressive stress–strain curves for aluminium alloy 2024 T 351 showing the influence of constraint to sideflow in increasing the effective flow stress. Curves represent simple compression (1), constrained compression (2), and punching from one side against a flat plate (3). The test geometry is shown schematically for each case.

The geometries of simple and constrained compression tests are shown schematically in Fig. 1, along with typical derived stress/strain curves for an aluminium alloy. The simple compression test, shown as curve 1 in Fig. 1, gives fundamental stress–strain data. The constrained compression test (Woodward and deMorton, 1976; Woodward, 1982) uses opposing cylindrical punches to indent and compress a plate of material and, as shown by curve 2 in Fig. 1, the derived stress–strain data are substantially different from the properties derived from the simple compression test, with the stress at any value of strain being much larger in the constrained test. This stress is a measure of resistance to indentation which also includes a small contribution due to the shear resistance of the material. The resistance to constrained compression is increased over that for simple compression by the surrounding plate which forms a barrier to extrusion to be overcome allowing yield and radial flow. The test is therefore a close measure of the real resistance of a plate to a penetrator under ballistic conditions, and the effective increase in flow stress due to the constraint can be estimated by simple plasticity models (Woodward and deMorton, 1976). The constrained compression test has been performed dynamically using the split Hopkinson bar (Liss *et al.*, 1983), and Crouch (private communication) has proposed that one-sided indentation may be a useful simplification. This method has been applied to composites (Culnane *et al.*, 1991), resulting in a slight change in the mechanics, particularly in relation to the contribution of shearing and slipping of the plate over the punch in the latter stages of penetration. Curve 3 in Fig. 1 shows that the stress–strain data obtained for a metal sample in one-sided constrained compression is comparable to that obtained when punching from both sides. One-sided indentation simplifies alignment considerably. Sample preparation for this test is trivial, a representative square of material with parallel faces being all that is required. This is particularly important for composite materials as there is no question of edge effects as would be the case if a small cylinder was used in a simple compression test. The sample is also considered representative of the bulk material as the lay-up can be oriented appropriately for penetration. This allows the development of deformation structures relevant to a plate-indentation problem. Constrained compression tests were performed quasi-statically with a 6.35 mm diameter hard cylindrical punch in a screw-type testing machine. For dynamic tests a 12.7 mm diameter direct impact Hopkinson bar (Wulf and Richardson, 1974) was used with a 6.35 mm diameter cylindrical tip ground onto the impact bar. Stress–strain computations were possible for times up to two return periods of transit of the elastic stress wave in the impactor bar. In the constrained compression test the stress resisting penetration is the

measured load divided by the punch cross-sectional area. The compressive strain is the natural logarithm of the instantaneous thickness of material between the punch and platen divided by the original plate thickness.

Samples deformed in ballistic testing and in compression were filled with an epoxy, which contained a dye to give optical contrast with undamaged material, then sectioned for examination (Culnane *et al.*, 1991).

Tensile tests were also performed on each of the composites using a screw-type testing machine with self-tightening jaws and dumbbell-shaped specimens to ensure failure occurred within the gauge length region. The test data presented, represent the mean of at least four tests. As shown in Tables 1 and 2, except for the GRP, composites tested for resistance to penetration and compression were laminated using different resins to those used for uniaxial tensile tests. The simple explanation is that during the time lag between manufacturing composite specimens for penetration/compression resistance and tensile strength, the A2785CV polyester resin was withdrawn from Australian manufacture. A readily available toughened vinylester resin was substituted for all specimens tested for uniaxial tension. Although using different resins is not ideal, the tensile results determined were considered satisfactory, as the primary objective of the resin matrix in tensile failure is to transfer stresses to the stronger fibre reinforcement which is the major contributor to the overall tensile strength. Previous constrained ballistic experiments by Song and Egglestone (1987) on Kevlar® and S2 Glass laminates encapsulated in Phenolic resin toughened with varying amounts of Polyvinylbutyral (PVB) (larger amounts of PVB giving toughest resins) showed only a 5% variation of perforation ballistic limit for 5- and 19-layer laminates, even though there were large differences in resin toughness. The small variation in ballistic efficiency is associated principally with deformation in the break-out phase during perforation. In the experiments considered in the present report, perforation is not involved, therefore the breakout phase has no influence. Hence the change in resin system is not considered to impact on the discussion of experimental results because it does not influence the property factors relevant to the penetration and constrained compression tests.

## BALLISTIC TEST RESULTS

Figure 2 shows sections of targets penetrated by flat-ended projectiles at similar velocities. The residual penetration depths allow a calculation of the mean pressure resisting penetration using eqn (1), and these values are listed in Table 3 with the highest resistance being shown by the GRP composite, the next highest by the Kevlar® and the least resistance by nylon. In the case of the Kevlar® composite the projectile was ejected by elastic rebound, indicating a significant elastic distortion for this material, not observed for the GRP or nylon. The calculated radius of fibre stretching, eqn (2), is also given in Table 3. Quasi-static tensile modulus and fracture strain data were used for these calculations; however, as discussed below, these values are consistent with dynamic data from the constrained compression tests.

Table 3. Resistance to penetration compared to compression test data

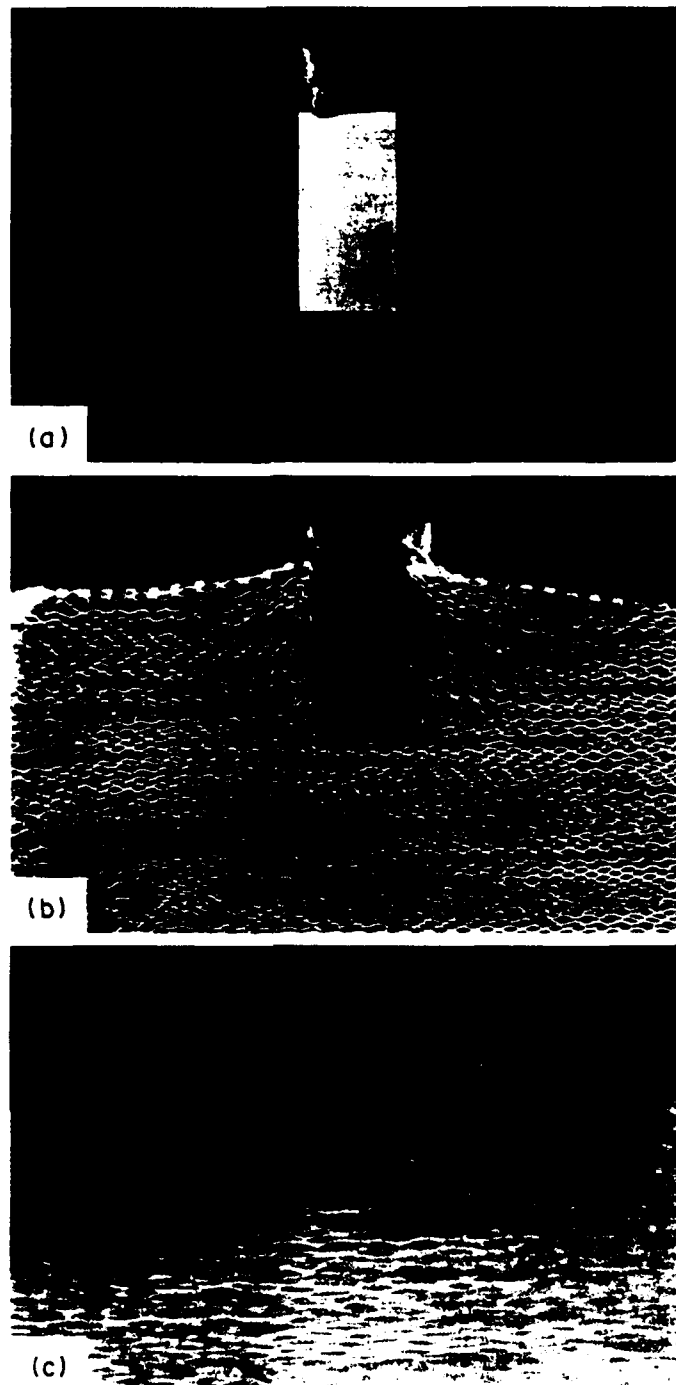| | | | Stress level in constrained compression (MPa) | | | |
| | | | Dynamic | | Quasi-static | |
| Material | Pressure resisting penetration (MPa) | Calculated radius of fibre stretching (mm) | Maximum | Mean following load drop | Maximum | Mean following load drop |
|---|---|---|---|---|---|---|
| GRP | 1190 | 107 | 750 | 570 | 1300 | 600 |
| Kevlar® | 615 | 38 | 1200 | 600 | 1200 | 700 |
| Nylon | 400 | 22 | 500 | 200 | 560 | 300 |
| Polyethylene | No result | No result | 650 | 200 | 970 | 320 |

Fig. 2. Sections of "semi-infinite" targets penetrated by flat-ended projectiles. (a) Nylon, 332 m s$^{-1}$, depth 27 mm. (b) Kevlar®, 336 m s$^{-1}$, depth 18 mm. (c) GRP, 330 m s$^{-1}$, depth 9 mm.
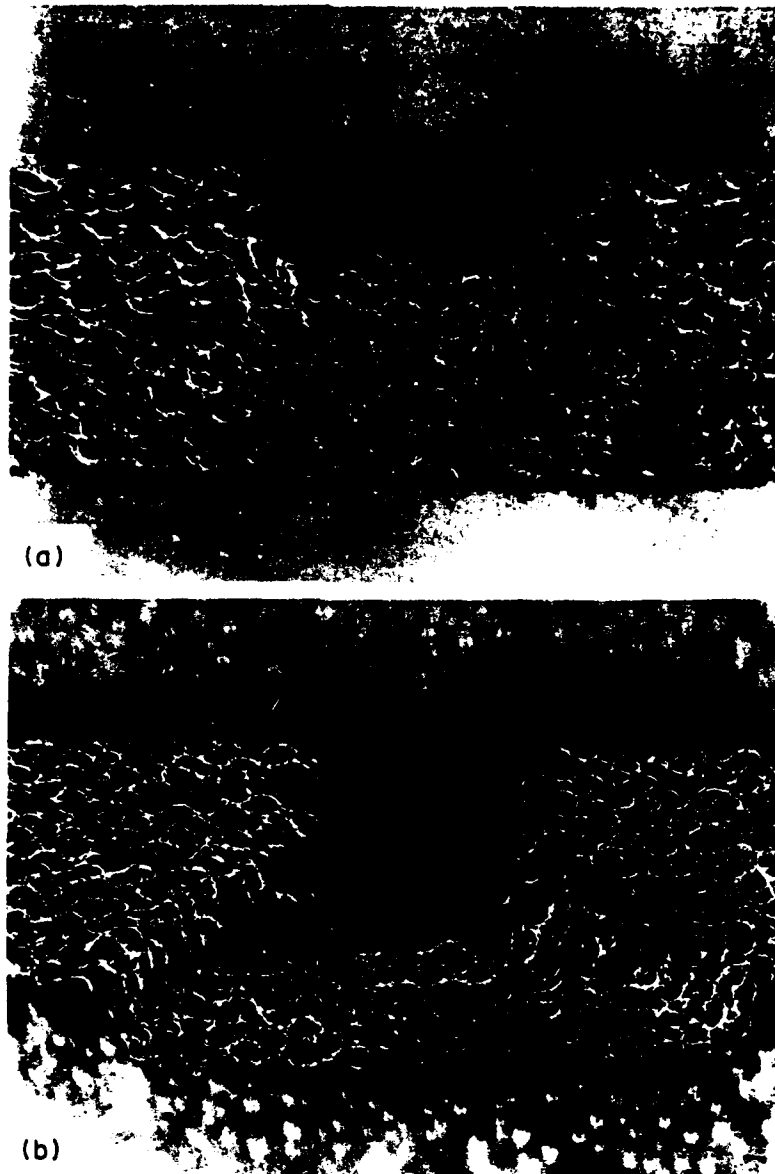
Fig. 5. Examples of wedge formation in quasi-statically compressed nylon composites showing extrusion of material away from the indenting punch. (a) Applied compressive strain = 0.41; (b) applied compressive strain = 0.81.
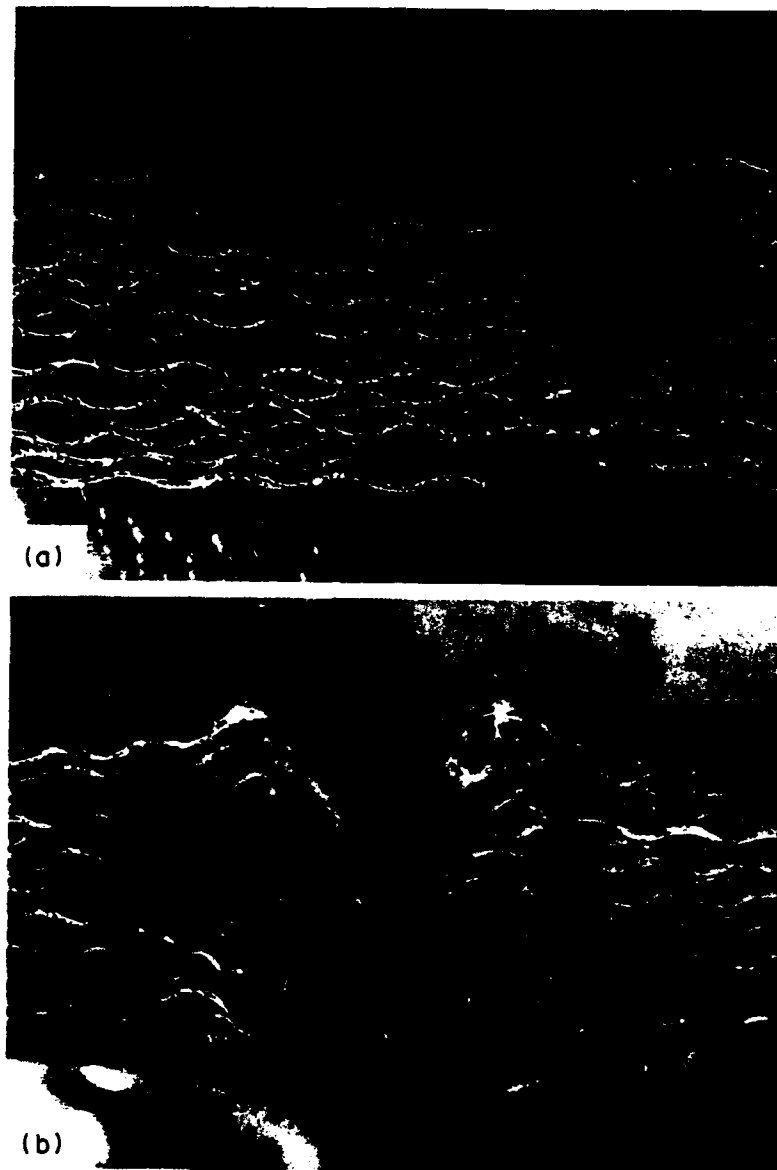
Fig. 6. Sections of Kevlar® composites after one-sided constrained compression showing upflow of material around the punch and fibres which have fractured, withdrawn and pushed to the side. (a) Applied compressive strain = 0.36; (b) applied compressive strain = 1.48.

The sectioned nylon composite target, Fig. 2(a), shows buckling of fibres below and beside the penetrator, consistent with fibre stretching and fracture ahead of the penetrator followed by extrusion to the side by the advancing penetrator. The buckling beneath the penetrator in this case is assumed to result from a small amount of elastic recovery as fibres bend and retract, curling up in the process. The Kevlar® composite shows evidence for a similar mechanism with buckling of fibres at the side of the penetrator and tensile fracture of strands immediately beneath. The buckling of fibres is, however, not evident directly below the penetrator, possibly because of the higher tensile strength of the Kevlar® and the substantial elastic recovery of the unbroken strands. The Kevlar® target also showed some delamination, evident in Fig. 2(b). The GRP target showed that fibre fracture and crushing of the composite occurs to about one-half projectile diameter ahead of the penetrator and extrusion of this material to the side causes a region of delamination and up-flow clearly evident from the sectioned dye/epoxy impregnated specimen. Greaves (1992) identified crushing ahead of the penetrator as a major energy-absorbing mechanism in the early stages of penetration of finite-thickness GRP targets. The calculated radius of stretched fibres for both nylon and Kevlar®, Table 3, is consistent with the radius to which buckling of fibres is observed in Figs 2(a) and 2(b), respectively, supporting strongly the contention that the impact energy is largely absorbed by fibre tension. The calculated radius for GRP, on the other hand, is much greater than the radius of the cracking and delamination evident for the thick GRP composite of Fig. 2(c), suggesting that fibre stretching cannot be the mechanism of energy absorption in this case.

## CONSTRAINED COMPRESSION RESULTS

Typical stress–strain curves for composites obtained from quasi-static and dynamic one-sided constrained compression tests are shown in Fig. 3. In the quasi-static tests the stress rises to a maximum and then drops to an intermediate level where it oscillates for Kevlar®, and remains steady for the GRP, polyethylene and nylon. In the dynamic tests the Kevlar®, polyethylene and nylon show stress–strain curves characteristically similar to their quasi-static behaviour, whereas for GRP the first drop in stress occurs at a much lower level in the dynamic test with the continued deformation being characterized by oscillations in the stress level.

Table 3 lists the values for the maximum stress in constrained compression and the mean lower level of stress (at which the sample continiued to deform after the drop in stress). These values are compared to the mean pressure resisting penetration as calculated from the penetration test. Results are not consistent with the high-penetration resistance of the GRP composite. To establish a mechanistic connection between the constrained compression test and penetration of semi-infinite targets, sectioned samples of the former were examined. Two basic mechanisms of deformation were observed, as illustrated in Fig. 4. In one case, Fig. 4(a), after composite compression and stretching of fibres, a wedge fracture appears. This wedge is pushed through the composite and is compressed, with parting and extrusion to the side of adjacent material, causing the sample to move up and around the punch. Such behaviour was observed for both nylon and GRP in quasi-static testing and typical examples are shown in Fig. 5. Note that there is little up-flow of composite material, and the extrusion from the back of the sample reduces confinement. The other characteristic type of behavior illustrated in Fig. 4(b) involves stretching, tensile fracture, and withdrawal by elastic recovery of fibre strands which are then pushed aside resulting in up flow around the punch. Characteristically, this behavior resulted in the fibres pulling out from beneath the punch as observed for Kevlar® and polyethylene composites in both quasi-static and dynamic tests. Examples are shown in Fig. 6. This type of behavior was also observed for nylon in the dynamic tests except that nylon had a tendency to form a small, wider-angle wedge. The GRP also behaved in this manner in the dynamic tests except that the fibres did not tend to withdraw, but were bent, fractured and extruded, with some unbroken strands springing back when the punch was removed.
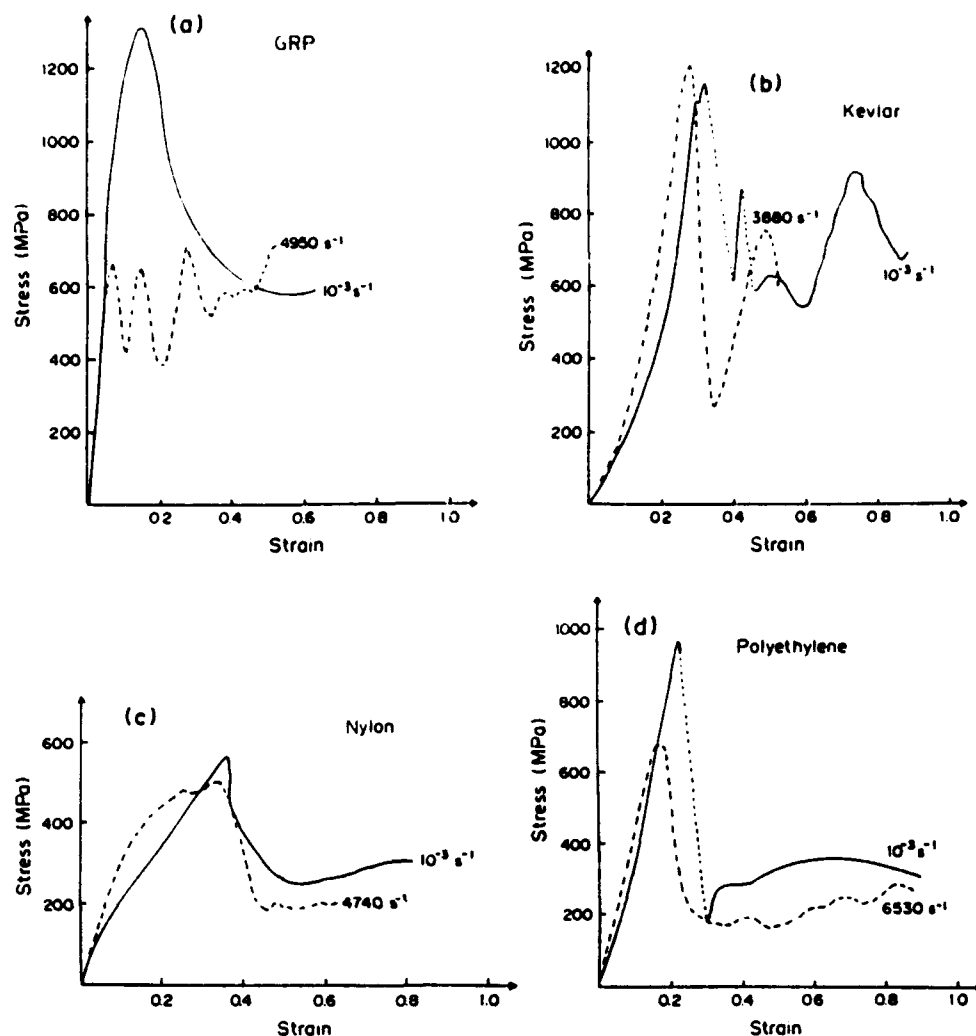
Fig. 3. Stress–strain curves for composites obtained in quasi-static and dynamic constrained compression tests. (a) GRP. (b) Kevlar®. (c) Nylon. (d) Polyethylene. Strain rates are indicated.

Interpretation of the stress–strain curves of Fig. 3 in terms of the mechanisms shown in Fig. 4 is not simple, especially as a change in mode for nylon when going from the quasi-static to the dynamic test is not reflected in a change in the stress–strain curve. For GRP and nylon composites tested quasi-statically, Figs 3(a) and 3(c), the drop from maximum load coincides with the development of a fracture and the continued deformation at the lower load is associated with extrusion of the fractured material against the radial confinement. For the Kevlar® composite, Fig. 3(b), the strain at which the first drop in load occurs represents an indentation of up to six layers of composite and hence substantial fibre stretching. The load shedding as fibres break results in an avalanche of fractures and a large stress relief. Continued straining results in further fibre stretching and repeated cycling of the load as groups of stretched fibres break. In some other cases where the mechanism is also fibre stretching and rupture, e.g. dynamic loading of nylon composites and loading of polyethylene composites, Figs 3(c) and 3(d), the stress never builds up again after the first major rupture of fibres, indicating that subsequent fracture of fibres is continuous but on a more individual basis. The lower stress at which the initial drop in load occurred for GRP in the dynamic tests compared to the quasi-static tests needs explanation. It is most likely attributable to the change in deformation mode from wedge formation in the quasi-static test to crushing of fibres ahead of the punch in the dynamic test. The resistance to the punch is then governed by resistance to radial extrusion and is thus similar to that corresponding part of the curve for the quasi-static test on GRP.
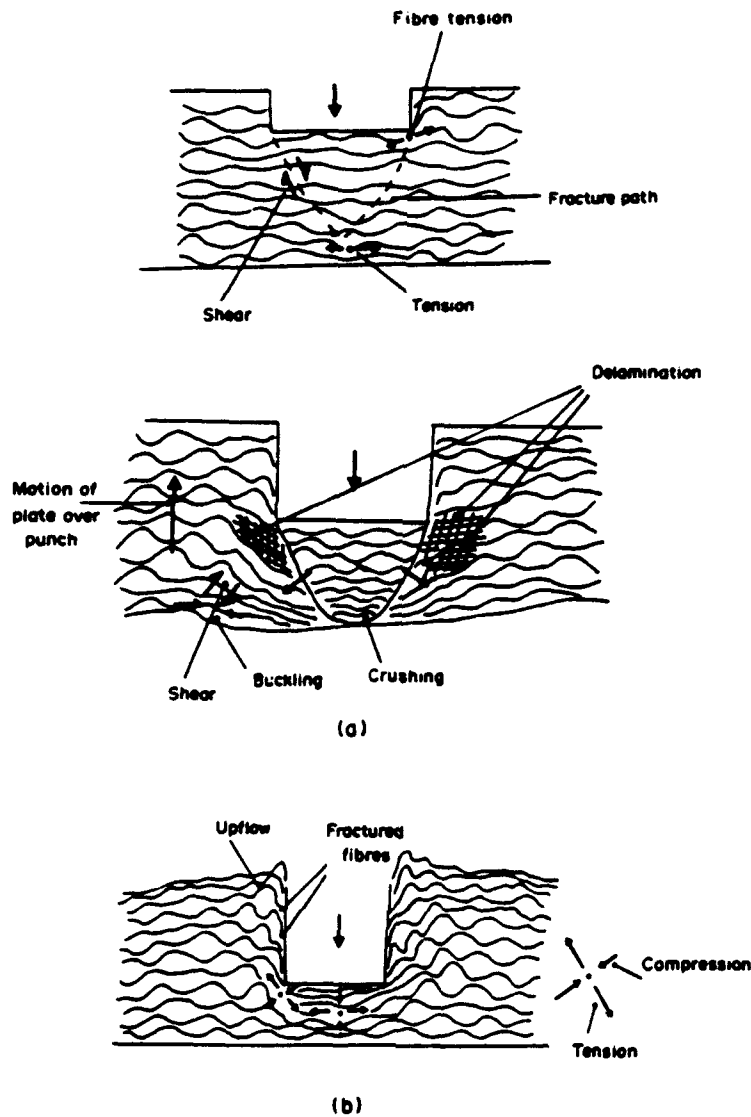
Fig. 4. Mechanisms of deformation in composites in one-sided constrained compression. (a) Composites which fracture to form a wedge and extrude material. (b) Composites in which fibres are stretched, fracture and withdraw.

## TENSILE TEST RESULTS

Mean values of tensile strength, elongation and tensile modulus are presented in Table 4. The GRP has a lower tensile strength and a lower tensile elongation than the Kevlar® composite; however, it has a higher tensile modulus. Reference to Fig. 3 will show that the compressive modulus of GRP is also higher than that of Kevlar® in the constrained compression test.

Table 4. Tensile test data

| Material | Tensile strength (MPa) | Elongation to rupture (%) | Tensile modulus (GPa) |
|---|---|---|---|
| GRP | 308 | 2.1 | 18.1 |
| Kevlar® | 399 | 5.2 | 12.0 |
| Nylon | 167 | 23.0 | 1.2 |
| Polyethylene | 751 | 7.4 | 16.6 |

## DISCUSSION

The sectioned penetrated targets suggest a fibre stretching, fracture, withdrawal by elastic recovery and extrusion mechanism for penetration, except for GRP which, in addition, shows some fibre and composite fragmentation ahead of the penetrator. These features are also observed in dynamic constrained compression tests, although some materials deform by the formation of a wedge and extrusion in equivalent quasi-static tests. Fracture strength and strain measurements give values which do not correlate directly with measured resistance to penetration. Tensile modulus does, however, correlate with resistance to penetration. For the nylon and Kevlar® composites, tensile fibre stretching appears to be the mechanism of energy absorption. The mechanism by which GRP composites absorb kinetic energy is less clear. An estimate of the elastic strain energy is $0.5E\varepsilon_f^2 V$, where $E$ is the modulus, $\varepsilon_f$ is the fracture strain and $V$ is the volume of material strained. The volume, $V$ calculated by equating elastic strain energy to impact energy, is much larger than that evident in the sectioned specimen of Fig. 2(c), because $\varepsilon_f$ is low for GRP. The quasi-static and dynamic constrained compression tests show that material properties are relatively strain-rate insensitive for all the composites used. In addition the dynamic fracture strain and dynamic modulus of GRP order the same way relative to the other composites as they do in the tensile tests. Mechanisms of deformation can, however, change radically with strain rate. At low strain rates some composites deform with the formation of a wedge followed by extrusion while at higher strain rates they fail by fibre tensile fracture.

Trying to group all the composites and develop a single model is not the most successful approach. It seems possible to group the organic-fibre composites as "ductile", with the resistance to penetration being governed by tensile strain energy absorption capability. Glass-fibre composites may be treated separately as "brittle", with resistance to penetration being governed by the difficulty in extruding crushed material from the path of penetration. This approach fits with the observations of Greaves (1992) on the penetration of GRP composites. GRP is the least ductile composite as judged by the failure strain in tension, as well as the initial fracture strain in both dynamic and quasi-static constrained compression tests. The higher resistance to penetration into the semi-infinite target, compared to the mean resistance to dynamic constrained compression, is probably a consequence of high confinement in the former, and confinement relieved to some extent by the ability of GRP to extrude from the back in the latter test. This effect of confinement with a thick composite would accord with the general observation (Hartman, 1986) that thin GRP targets show less resistance to perforation than Kevlar® composites, but the relative performance is reversed with thick composites. In a thin target a mechanism for extrusion is more easily developed. In a thick composite the extrusion of crushed fibre and matrix requires elastic compression of the surrounding material. For a metal, which deforms plastically, mechanisms for large shear displacement which maintain continuity are available. For these composite materials, large displacements can occur by delamination and bending or by shear along fractures. The extrusion of GRP appears to involve delamination and bending in Fig. 2(c). The problems of extrusion suggest that projectile diameter and nose shape will be important parameters in the penetration of GRP composites. The characteristics which lead to the different behavior of GRP are low-fracture strain leading more readily to multiple fractures, better bonding between the fibre and matrix making fibre stretching and pull-out more difficult, and high elastic modulus resulting in high stress levels at small strains.

This work clearly highlights the need to study deformation mechanisms of composites in some detail in order to develop suitable models which relate strength properties in simple tests to observed behaviour in complex loading situations. The individual characteristics of the fibre type make it difficult to establish a general pattern. In understanding the ballistic impact of fibre composites, simple tests designed to emulate elements of the deformation history are only useful if the correspondence with ballistic impact is clearly established in relation to fibre and matrix distortion and fracture mechanisms.

## CONCLUSION

This work has tested GRP, Kevlar®, nylon and polyethylene laminates for resistance to ballistic penetration, compression in constrained compression tests and tensile failure. It was demonstrated that the mechanism of ballistic penetration is by stretching, fracture, withdrawal by elastic recovery and extrusion of fibres, except for GRP where crushing fracture of the composite occurs immediately ahead to the penetrator. These mechanisms are also observed in dynamic constrained compression tests. For nylon and GRP quasistatic constrained compression tests produce a different deformation mechanism, the formation of a wedge by fracture, followed by compression of the wedge and extrusion of adjacent material. Fracture strength and ductility measures do not correlate with ballistic resistance unless the GRP is treated as a separate case to the organic composites. Fibre crushing is the distinguishing mechanism for the GRP composites. A correlation was found to exist between tensile modulus and ballistic resistance. Properties which are linked to the different behavior of GRP composites are the low fracture strain, high tensile modulus and good bonding between the fibre and the matrix.

## REFERENCES

Ayez, M. E., Roux, M. R. and Moureaud, M. J. (1991). Rupture dynamique de stratifies fibre de verre. *J. de Physique IV*, Colloque C3, Suppl. au. *J. de Physique III* 1, C3-687–C3-692.

Culnane, A. H., Woodward, R. L. and Egglestone, G. T. (1991). Failure examination of composite materials using standard metallographic techniques. *J. Mat. Sci. Lett.* 10, 333–334.

Crouch, I. G. and Woodward, R. L. (1989). The use of simulation techniques to study perforation mechanisms in laminated metallic composites. Inst. Phys. Conf. Ser. No. 1–2, *Int. Conf. on Mechanical Properties of Materials at High Rates of Strain*, Oxford (Edited by J. Harding), pp. 481–488. Institute of Physics, Bristol.

Egglestone, G. T., Gellert, E. P. and Woodward, R. L. (1990). Perforation failure mechanisms in laminated composites. In *Materials United in the Service of Man* (Edited by R. D. Davies and D. I. Hatcher), *Proc. Inst. Metals and Materials Australasia, Annual Conf.*, Perth, WA, Sept. 1990, Vol. 1, pp. 1-2.1–1-2.11. Institute of Metals and Materials Australasia.

Greaves, L. J. (1992). Failure mechanisms in glass fibre reinforced plastic armour. DRA Military Division Memorandum 12/92, Chertsey Memorandum 92003, Defence Research Agency, Chertsey, Surrey, March 1992.

Hartman, D. R. (1986). Ballistic impact behavior of high-strength glass-fibre composites. *Proc. 41st Annual Conf. Reinforced Plastics/Composite Institute*, p. H05, Session 16-D. The Society of Plastics Industry, 27–31 Jan.

Liss, J., Goldsmith, W. and Hauser, F. E. (1983). Constraint to side flow in plates. *Trans. ASME, J. Appl. Mech.* 50, 694–698.

Morrison, C. E., and Bowyer, W. H. (1980). Factors affecting the ballistic impact resistance of Kevlar laminates. *3rd Int. Conf. on Composite Materials, Advances in Composite Materials* (Edited by A. R. Bunsell), p. 233–245. Pergamon Press, New York.

O'Donnell, R. G. (1994). Deformation energy of Kevlar backing plates for ceramic armours. Submitted to *J. Mat. Sci.*

Savage, G. M. (1990). Fabric and fibre reinforced laminate armours. *Metals Mater.* 5, 285–290.

Song, J. W. and Egglestone, G. T. (1987). Investigation of the PVB/PF ratios on the crosslinking and ballistic properties in glass and aramid fibre laminate systems. *Proc. 19th Annual SAMPE Conf. on The Nation's Future Material Needs*, Anaheim, U.S.A., pp. 108–119. SAMPE, Covina, CA.

Woodward, R. L. (1982). Penetration of semi-infinite metal targets by deforming projectiles. *Int. J. Mech. Sci.* 24, 73–87.

Woodward, R. L. and Crouch, I. G. (1989). Ballistic perforation of laminated metallic composites—an approach to modelling. *Proc. 11th Int. Symp. on Ballistics*, Brussels, Belgium, Royal Military Academy, May 1989, Vol. II, p. 301–310.

Woodward, R. L. and deMorton, M. E. (1976). Penetration of targets by flat ended projectiles. *Int. J. Mech. Sci.* 18, 119–127.

Woodward, R. L., and Tracey, S. R. and Crouch, I. G. (1991). The response of homogeneous and laminated metallic sheet material to ballistic impact. *J. de Physique IV*, Colloque C3, Suppl. au. *J. de Physique III* 1, C3-277–C3-282.

Wulf, G. L. and Richardson, G. T. (1974). The measurement of dynamic stress-strain relationships at very high strains. *J. Phys. E.: Scient. Instrum.* 7, 167–169.

Zhu, G., Goldsmith, W. and Dharan, C. K. H. (1992). Penetration of laminated Kelvar by projectiles—I. Experimental investigation. *Int. J. Solids Structures* 29, 399–420.